

The response of summer monsoon onset/retreat in Sumatra-Java and tropical Australia region to global warming in CMIP3 models

Huqiang Zhang · A. Moise ·
Ping Liang · L. Hanson

Received: 18 October 2011 / Accepted: 3 May 2012 / Published online: 15 May 2012
© Springer-Verlag 2012

Abstract In this study, we assess the potential changes in the onset, retreat and duration of austral summer monsoon covering the domain from south Sumatra and Java region in the tropics to the northern Australian continent. We simply call it the Australian summer monsoon. Daily precipitable water and 850 hPa wind from 13 CMIP3 models are used in the diagnoses. A majority of the models can capture the northwest–southeast evolution of the summer monsoon, which starts from the south Sumatra and Java region around later November and then progressively approaches the Australian continent in late December. Nevertheless, significant biases exist in the modeled onset/retreat dates and the extent of the monsoon inland penetration. Under global warming, the agreement among the model projections varies across the domain. In between the Sumatra-Java archipelago and the top end of the Australian continent, over 80 % of the models simulate delayed monsoon onset and shortened duration by ~ 10 days, but less model agreement is seen over interior continent where the model ensembles show an approximate 7-day delay of both the onset and retreat with relatively little change in duration. Both El Niño-Southern Oscillation and Indian Ocean SST patterns appear to play important roles in determining the variations of the modeled monsoon onset. Nevertheless, the extent of their influence varies significantly across the models. Under global warming, a large proportion of

models show relatively less warming in the eastern Indian Ocean and with a consequent increase in the modeled Indian Ocean Dipole index. Both a weakened and/or eastward shift of the upward branch of Walker circulation and the Indian Ocean contribute to the simulated delayed onset and shortened duration in the tropics under global warming.

1 Introduction

The austral summer monsoon occurring over the southern part of the maritime continent and tropical Australia is part of the large-scale Australia-Asia monsoon system extending from East Asia to northern Australia (Chang and Krishnamurti 1987; Wang 2006; Wheeler and McBride 2005, 2006). As the counterpart to “Asian monsoon” named for the Northern Hemisphere component, here we simply call the austral summer monsoon component as the Australian summer monsoon. It refers to the rapid rainfall and circulation transitions from dry to wet climate during austral late spring to summer in the domain covering the northern part of the Australian continent and extending northward up to a large part of the Indonesia archipelago including south Sumatra, the Java and Timor region and nearby waters (Moron et al. 2009). Its onset is accompanied by the reversal of low-level easterly trade winds into west to northwesterly winds which generate deep convection and heavy rainfall in the monsoon trough region (Wheeler and McBride 2005). The moisture-laden westerly winds originate from the tropical Indian Ocean and southern Asian waters. Accordingly, the onset of the summer monsoon wet season often starts from late September to early October in the southern Indonesia region from south Sumatra to Timor Island and nearby waters (Aldrian and Susanto 2003; Moron et al. 2009), progresses southeastward and reaches northern

H. Zhang (✉) · A. Moise · L. Hanson
Centre for Australian Weather and Climate Research,
A Partnership Between the Australian Bureau of Meteorology
and CSIRO, GPO Box 1289k, Melbourne, VIC 3001, Australia
e-mail: h.zhang@bom.gov.au

P. Liang
Shanghai Regional Climate Center,
China Meteorological Administration, Shanghai, China

Australia in late December (Hendon and Liebmann 1990; Drosowsky 1996; Smith et al. 2008; Zhang 2010). Through the strong cross-equatorial flow over the southeast Asia region, the Australian summer monsoon is linked to its Asian counterpart, with studies such as Chang et al. (1979), Sumi and Murakami (1981), Chen et al. (1991) and Zhang and Zhang (2010) showing the influence of the Asian winter monsoon on the development of the Australian summer monsoon.

Studying the onset and retreat of the Australian summer monsoon has long been an active research area (e.g. Troup 1961; Nicholls et al. 1982; Nicholls 1984; Holland 1986; Hendon and Liebmann 1990; Joseph et al. 1991; Drosowsky 1996; Smith et al. 2008; Kajikawa et al. 2009) as such pronounced rainfall variations have profound social and economic impacts (e.g. Moron et al. 2009). Nevertheless, as pointed out by Kajikawa et al. (2009) and Zhang (2010), a large number of the previous studies were based on the analysis of rainfall and/or wind data from Darwin, or using area-averaged wind data over a specific region (e.g. Webster 2006; Kajikawa et al. 2009). These studies did not describe the detailed spatial and temporal evolution of the monsoon development such as time of its development, the speed and direction of its southward penetration etc. Only in the last several years have a number of studies used gridded rainfall, wind or moisture data over the continent to examine these details (e.g. Zeng and Lu 2004; Smith et al. 2008; Zhang 2010).

As reviewed in detail in Drosowsky (1996) and Smith et al. (2008), there has been a variety of monsoon onset/retreat definitions used in previous studies. Each definition has its own merits in capturing some characteristics associated with the monsoon. With the intention of developing a monsoon onset/retreat definition which could allow a study of detailed monsoon features simulated by global climate models, Zhang (2010) combined the method of Li and Zeng (2003) and Zeng and Lu (2004) in using both the 850 hPa wind and atmospheric volumetric precipitable water (*PW*) to derive monsoon onset/retreat. The rationale behind this definition is twofold: (1) these two variables capture the fundamental processes governing the monsoon, namely the moisture condition represented by *PW* and the dynamical condition represented by the 850 hPa wind; (2) global climate models with their current resolution and configuration have some skill in simulating these two large-scale variables, while they often show significant errors in rainfall simulations (e.g. Colman et al. 2011). For instance, Moise and Colman (2009) found that CMIP3 models had some deficiencies in simulating the twentieth Century monthly mean rainfall climatology but that some of the large-scale features such as zonal wind were reasonably simulated over the tropical Australian region. Using daily *PW* and wind data from ERA-40 reanalysis

data, Zhang (2010) also showed good agreement between simulated monsoon onset dates with the onset dates diagnosed from observed rainfall and/or wind data over Australian (Drosowsky 1996; Smith et al. 2008).

Assessing the potential impacts of global warming on the global monsoon system has long been the focus of climate change studies using the results of coupled climate model simulations. As reviewed in Zhang et al. (2012), a number of studies have been dedicated to the Asian monsoon (e.g. Kitoh and Uchiyama 2006; Kim et al. 2008; Lin et al. 2008; Li et al. 2010), but relatively few have focused on the Australian monsoon (e.g. Colman et al. 2011; Moise et al. 2012). Furthermore, most studies only used monthly model outputs so only aspects related to monsoon mean climate and its intra-seasonal, seasonal and interannual variations were investigated. In recent years, studies have used daily model outputs to analyze monsoon onset/retreat and duration which are critical to draw a full picture of how monsoon evolves in the future climate. For instance, Kitoh and Uchiyama (2006) used 20-year daily rainfall data to estimate the model-simulated changes in the onset/retreat of the Asian monsoon rainy season. They found weak changes in onset dates, relatively bigger changes in retreat dates, and different features in the western North Pacific, southern China and the Indochina peninsula. Nevertheless, as there was no consideration of the monsoon circulation in their definition, some of these changes were not monsoon related (ref Zhang et al. 2012).

Over the Australian monsoon domain, most studies have used monthly data to analyze changes in mean rainfall, temperature and circulation. For example, Colman et al. (2011) analyzed the skill of a suite of CMIP3 models in reproducing the broad features of observed rainfall, temperature and circulation variations over northern Australia. They showed significant divergence in terms of the model skill, with half the models overestimating the tropical rainfall and the other half underestimating it. The seasonal reversal of the monsoon circulation in the region and the location, orientation and seasonal progression of the low-level monsoon “shear line” were found to be reasonable in the model ensemble mean, but with varying skill in each of the individual models. Subsequently, Moise et al. (2012) showed significant uncertainties in the CMIP3 model-simulated changes in mean climate in the tropical Australian region. While the overall changes in rainfall in tropical Australian rainfall were small, the small increases in March and April led them to suspect a simulation of a prolonged Australian monsoon. However, they found this increase was largely due to thermodynamic effects associated with enhanced atmospheric moisture content and that the dynamic effects contributed to a weakened monsoon circulation. The ability of models to simulate the onset of the monsoon season, its intensity and durations and their

potential changes in global-warmed climate has not been addressed to date.

Here, we apply the method of Zhang (2010) to a suite of CMIP3 models to study potential changes in Australian summer monsoon onset and retreat in a global-warmed climate. Zhang et al. (2012) have carried out a similar analysis over the Asian summer monsoon region. In Sect. 2, we briefly introduce the CMIP3 models and their simulations used in this analysis. The method of Zhang (2010) used to define the Australian summer monsoon onset/retreat is briefly described. Main results will be presented in Sect. 3 including (1) the model skills in reproducing observed features (derived from ERA-40 reanalysis data); (2) projected changes in monsoon onset/retreat simulated by the models, and (3) dominant processes operating in these models. Finally, Sect. 4 summarizes and discusses the main findings from this analysis.

2 Brief descriptions of CMIP3 models and monsoon onset definition

The models used in this study are 13 coupled climate models from the World Climate Research Programme (WCRP) Coupled Model Intercomparison Project phase 3 (CMIP3, Meehl et al. 2007) multi-model dataset, otherwise known as “IPCC AR4” models as these model results were heavily used in the IPCC AR4 report (Solomon et al. 2007). The models are the same as used in Zhang et al. (2012) and are selected based on daily data availability and their broad skill in reproducing the observed Australian summer monsoon

rainfall distribution. Some CMIP3 models were excluded because of poor simulations of summer monsoon rainfall. Table 1 gives a brief model description (further details can be obtained from the PCMDI CMIP3 data website: http://www-pcmdi.llnl.gov/ipcc/about_ipcc.php). The models differ significantly in their configurations, with horizontal resolutions in their atmospheric components varying from about $1^\circ \times 1^\circ$ to $4^\circ \times 5^\circ$ and vertical levels from 18 to 56 levels. There are also large variations in the model key parameterizations and coupled ocean model configurations. These variations in model configuration can contribute to significant variations in the skill of the models in reproducing the mean tropical climate in the region (e.g. Colman et al. 2011). In this study, we have analyzed three sets of CMIP3 model experiments: 20C3 M for twentieth century climate and SRESA1B (hereafter referred as A1B) and SRESA2 (hereafter referred as A2) for two different twenty-first century emission scenarios, with A2 having higher emissions than A1B. Because of the size of the datasets used for the analysis, we have analyzed only one ensemble member from each of the model runs for 20-year periods covering 1981–2000 in 20C3 M, and 2081–2100 for A1B and A2. Overall, we found very similar results from the A1B and A2 experiments and therefore only present the A2 results when we discuss monsoon changes under global warming.

Considering that the start of the monsoon rainy season is accompanied by the rapid establishment of a monsoon westerly circulation and a significant moistening of the atmosphere, Zhang (2010) combined the method of Zeng and Lu (2004) and Li and Zeng (2003) and used both the 850 hPa winds and atmospheric volumetric precipitable

Table 1 CMIP3 models analysed in this study

Model name	Modelling group	Atmospheric resolution	Ocean resolution
bccr_bcm2_0	Bjerknes Centre for Climate Research, Norway	T63 ($1.9^\circ \times 1.9^\circ$) L31	$0.5^\circ\text{--}1.5^\circ \times 1.5^\circ$ L35
cnrm_cm3_1	Meteo-France/Centre National de Recherches Meteorologiques, France	T63 ($\sim 1.9^\circ \times 1.9^\circ$) L45	$0.5^\circ\text{--}2^\circ \times 2^\circ$ L31
csiro_mk3_0	CSIRO Atmospheric Research, Australia	T63 ($\sim 1.9^\circ \times 1.9^\circ$) L18	$0.8^\circ \times 1.9^\circ$ L31
csiro_mk3_5	CSIRO Atmospheric Research, Australia	T63 ($\sim 1.9^\circ \times 1.9^\circ$) L18	$0.8^\circ \times 1.9^\circ$ L31
gfdl_cm2_0	Geophysical Fluid Dynamics Laboratory, USA	$2.0^\circ \times 2.5^\circ$ L24	$0.3^\circ\text{--}1.0^\circ \times 1.0^\circ$
gfdl_cm2_1	Geophysical Fluid Dynamics Laboratory, USA	$2.0^\circ \times 2.5^\circ$ L24	$0.3^\circ\text{--}1.0^\circ \times 1.0^\circ$
ingv_echam4	Instituto Nazionale di Geofisica e Vulcanologia, Italy	T106 ($\sim 1.1^\circ \times 1.1^\circ$) L19	$2^\circ \times 2^\circ$ L31
innmcm3_0	Institute for Numerical Mathematics, Russia	$4^\circ \times 5^\circ$ L21	$2^\circ \times 2.5^\circ$ L33
ipsl_cm4	Institut Pierre Simon Laplace, France	$2.5^\circ \times 3.75^\circ$ L19	$2^\circ \times 2^\circ$ L31
miroc3_2_medres	Center for Climate System Research (University of Tokyo) and Frontier Research Center for Global Change, Japan	T106 ($\sim 1.1^\circ \times 1.1^\circ$) L56	$0.2^\circ \times 0.3^\circ$ L47
miub_echo_g	Meteorological Institute of the University of Bonn (Germany/Korea)	T30 ($3.75^\circ \times 3.75^\circ$) L19	$0.5^\circ\text{--}2.8^\circ \times 2.8^\circ$ L20
mpi_echam5	Max Planck Institute for Meteorology (Germany)	T63 ($\sim 1.9^\circ \times 1.9^\circ$) L31	$1.5^\circ \times 1.5^\circ$ L40
mri_cgcm2_3_2a	Meteorological Research Institute, Japan	T42 ($\sim 2.8^\circ \times 2.8^\circ$) L30	$0.5^\circ\text{--}2.0^\circ \times 2.5^\circ$ L23

Detailed information on the model configurations can be obtained at the webpage: http://www-pcmdi.llnl.gov/ipcc/about_ipcc.php

water (PW) to define monsoon onset/retreat. In this method, normalised daily PW_n is calculated to capture the rapid atmospheric moistening prior to the summer monsoon onset:

$$PW_n = \frac{(PW - PW_{min})}{(PW_{max} - PW_{min})} \quad (1)$$

where PW_{max} and PW_{min} are the multi-year mean of daily PW maximum and minimum. $PW_{max} - PW_{min}$ measures the seasonality of daily PW . Monsoon onset is defined as follows: (1) PW_n exceeds a particular threshold (0.65) for three continuous days for at least 7 of the 9 adjacent points around a location. Zhang (2010) pointed out that the results were not sensitive to different thresholds around 0.65; (2) an 850 hPa monsoon westerly is established: defined as the averaged zonal wind of the 9 adjacent points around the location remaining westerly for three consecutive days. Monsoon duration is defined as the difference between the onset and retreat dates. The detailed method is outlined in Zhang (2010) and Zhang et al. (2012). In the analysis, the model-simulated daily PW is derived as the vertically integrated atmospheric specific humidity. Normalized PW_n is calculated using the model PW_{max} and PW_{min} for the 20-year periods of 1981–2000 (from 20C3 M) and 2081–2100 (from A2). Note that the Australian monsoon typically spans two calendar years, so there are only 19 onset/retreats during the each period.

According to the Clausius-Clapeyron relationship (Wentz et al. 2007), atmospheric precipitable water increases with air temperature because more water vapor can be held in the air. Thus, one would expect that global warming would systematically increase PW and consequently result in an earlier monsoon onset according to the definition used here. Zhang et al. (2012) found that by using normalized PW (PW_n), which measures the moistening process associated with monsoon onset rather than PW itself, uniformed warming did not lead to uniform changes in monsoon onset/retreat in the Asian monsoon region. Nevertheless, using both PW_n and 850 hPa wind allows us to better understand the projected changes in monsoon characteristics in terms of changes in atmospheric circulation and moisture conditions.

3 Monsoon onset/retreat and their potential changes

3.1 Model-simulated monsoon in current climate

Figure 1 shows average monsoon onset dates from the 13 models based on their 20C3 M simulations over the 20-year period 1981–2000. We only show results over locations where the monsoon duration is longer than 5 days

and where there are more than 9 out of the 19 years during which monsoon onset is diagnosed. Results are compared with these based on the ERA-40 reanalysis data for the same period (Fig. 1o).

The evolution of the summer monsoon onset in this region is reasonably simulated by the majority of the CMIP3 models. As noted by Moron et al. (2009), the onset of the summer monsoon south of the equator has a northwest-to-southeastward progression pattern. To illustrate this feature, Table 2 compares averaged onset dates in each model at the grid points along a northwest–southeast transect from (5°S, 110°E) to (20°S, 140°E), including the results from the 13-model ensemble mean and the reanalysis. At each grid along the transect, the onset dates are averaged over 10° longitude band centered by this grid. In the reanalysis data, the monsoon starts from southern Sumatra and nearby warm waters around Julian Day (JD) 336. Note that this is also the location where cross-equatorial flow is strongest in the region (Zhang and Zhang 2010), suggesting a potential linkage between the Australian summer monsoon and the Asian winter monsoon in the Northern Hemisphere (Chang et al. 1979; Zhang and Zhang 2010). The monsoon then penetrates southeastward towards Java and Java Sea around JD 345 and progresses towards Timor and Timor Sea area around JD 352. Around JD 360 it reaches the warm water north of the Australian continent, then approaches the continent and moves further southeastward around JD 375. The 13-model ensemble gives remarkably similar dates to the ones derived from ERA-40. Nevertheless, such a good agreement between the model ensembles and the reanalysis does not mean the majority of the models simulate a similar monsoon onset date to the reanalysis results. In fact, there are large disagreements, with some models simulating much earlier onset by as much as 20–25 days while some simulating a later onset by about 30 days. These discrepancies are seen in the Australian rainfall analysis by Colman et al. (2011). Two outliers are the INGV model (Fig. 1g) which indicates a considerably early onset and much larger domain where monsoon occurs, and the CNRM model (Fig. 1b) which has a delayed onset. In CNRM, it appears that the Australian monsoon onset first occurs over the northern Australian land area. The reason for this could be linked to pre-monsoon thermal lows over the continent as discussed by Kim et al. (2006) in which the pre-monsoon continental warming was identified as a key factor for the monsoon onset. Among the 13 models, IPSL (Fig. 1i) and MRI (Fig. 1m) simulate the least inland penetration of the summer monsoon into the Australian continent. Correspondingly, these models also produced significant errors in their mean rainfall climatology over the region (not shown).

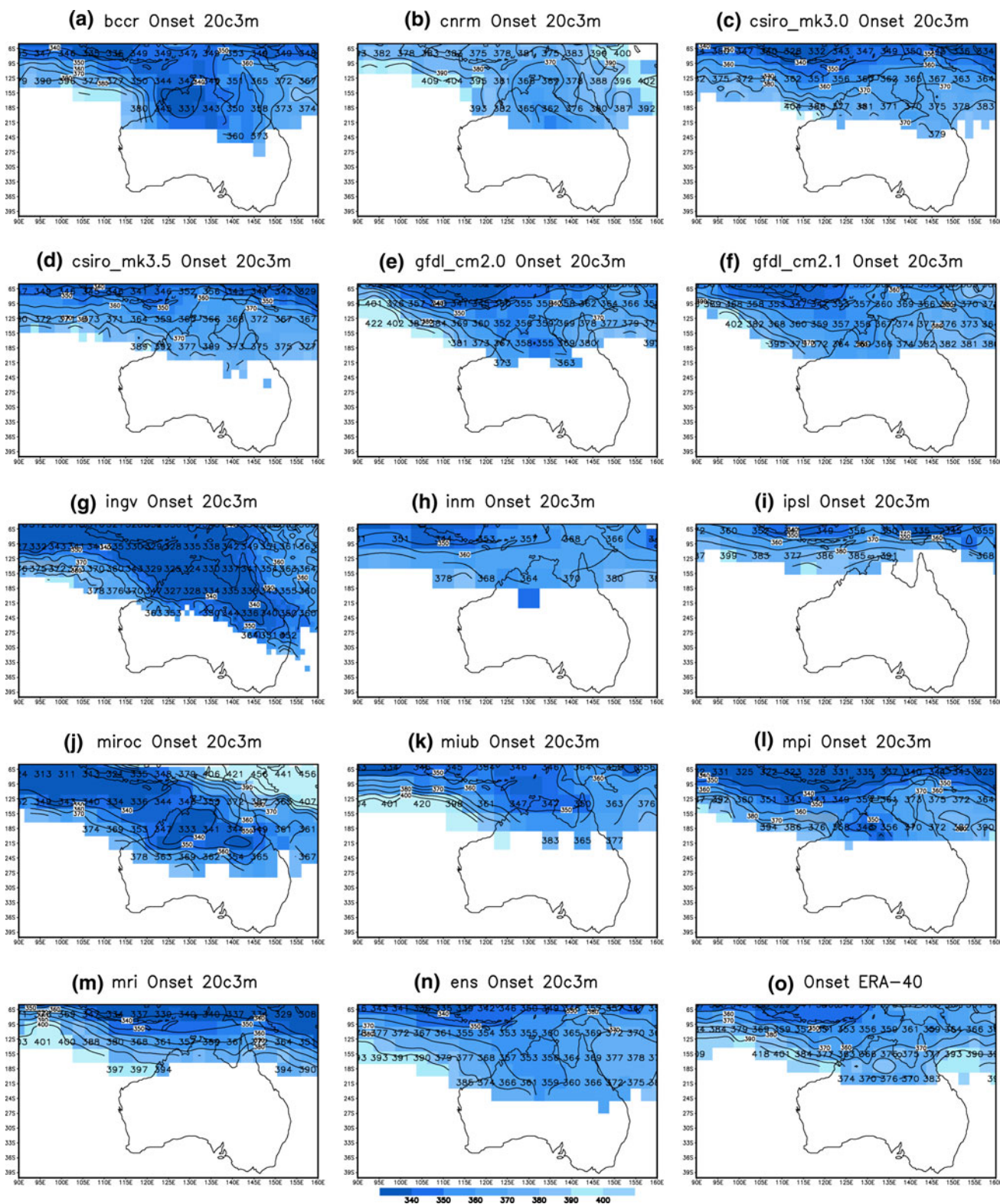


Fig. 1 a–m 19-year mean climatology of Australian monsoon onset dates (Julian day number) simulated by 13 CMIP3 models in their 20C3 M simulations over the period of 1981–2000. The model names are as listed in Table 1. Only locations where at least ten onsets have

occurred in the 19-year period are plotted. **n** 13-model ensemble results after regridding the model data to common 2.5° by 2.5° resolution; **o** averaged onset dates derived from the same method using 43-year ERA-40 reanalysis data for the period of 1959–2001

Table 2 Averaged onset dates (Julian Day, JD) at grid points along a northwest–southeast transect (starting from 5°S 110°E to 20°S 140°E) in the Australian monsoon region in the model 20C3 M runs

Model	5°S 105–115°E	7.5°S 110–120°E	10°S 115–125°E	12.5°S 120–130°E	15°S 125–135°E	17.5°S 130–140°E	20°S 135–145°E
bccr	313	339	345	346	340	346	350
cnrm	378	378	377	374	367	362	358
csiro mk3.0	326	340	349	356	371	373	368
csiro mk3.5	335	354	354	360	370	371	377
gfdl_cm2.0	316	331	346	355	355	357	360
gfdl_cm2.1	332	340	350	356	362	368	376
ingv	314	328	330	328	322	331	337
inm	342	347	351	366	363	366	
ipsl	345	344	367	386	393		
miroc	331	329	330	344	335	338	339
miub	345	353	353	354	357	356	374
mpi	322	331	339	350	352	350	360
mri	320	334	348	360	379		
ensemble	337	345	354	358	355	357	361
ERA-40	336	345	352	360	369	379	374

Results are averaged over 10° zonal band at each location

The monsoon duration dates are compared with ERA-40 reanalysis (Fig. 2). Similar to the onset dates, the 13-model ensemble gives reasonable results (Fig. 2n) compared with the results from ERA-40 reanalysis (Fig. 2o), particularly over the tropical oceans and northern Australia. Most models indicate a duration of about 100–120 days over the southern Indonesia archipelago, while the duration is about 50–70 days over most of northern Australia. Again, there are notable inter-model differences. For models with a weak monsoon such as INM (Fig. 2h) and IPSL (Fig. 2i), the duration is considerably shorter and the monsoon retreats about one month earlier over the tropics than in the reanalysis data.

3.2 Projected changes in monsoon onset and duration

To assess the potential changes in monsoon onset/retreat in a future climate, we analyze the results for the period of 2081–2100 (A2 experiments) relative to these from their 20C3 M experiments. While Zhang et al. (2012) found considerable model divergence in their projections of the Asian monsoon, Fig. 3 shows relatively better agreement for the change in the Australian monsoon onset. Except for three models (GFDL_CM2.0, GFDL_CM2.1 and MIUB), the majority of the models simulate a delayed onset over a large part of the summer monsoon domain (Fig. 3o), with over 80 % consistence in the tropics and above 60 % over northern Australia. The averaged delay of onset is about 7–10 days (Fig. 3n) over a large part of the region. Within the three outliers (GFDL_CM2.0, GFDL_CM2.1 and

MIUB), the GFDL two show mixed features, while MIUB (Fig. 3k) suggests the onset gets earlier by about 10–20 days. We will later discuss the reasons for such model disagreements.

As we only have 19 monsoon onset dates for each of the 20-year period, from such a small sample size it is difficult to derive meaningful and reliable statistical significance tests and sometime such significance tests could be rather misleading (ref. Nicholls 2000). However, considering that Australian monsoon onset has remarkable interannual variations (e.g. Drosowsky 1996; Smith et al. 2008; Zhang 2010), we further compare the time series of onset dates from the two experiments to assess the robustness of the changes in Fig. 3. Figure 4 shows the results averaged over the northern Australia (120–140°E and 17.5–10°S) where a number of models produce big changes but lack of agreement. Comparing Fig. 4 with Fig. 3 indicates that for models which show significant changes in mean onset dates, they are more likely to show notable changes in the time series of the onset dates in their 20C3 M and A2 experiments. For example, the time series from the models including BCCR, CSIRO_mk3.0, CSIRO_mk3.5, INGV, MIROC and MRI exhibit discernable shifts towards about 1-week delay. For the MIUB model which simulates significant early onset in Fig. 3k, there is also a systematic shift in the time series in Fig. 4k towards an early onset by about 10 days. For models which show mixed signal of changes in mean onset dates in Fig. 3, there are no distinguishable changes in the time series such as the ones from the two GFDL models, the IPSL and MPI. The multi-

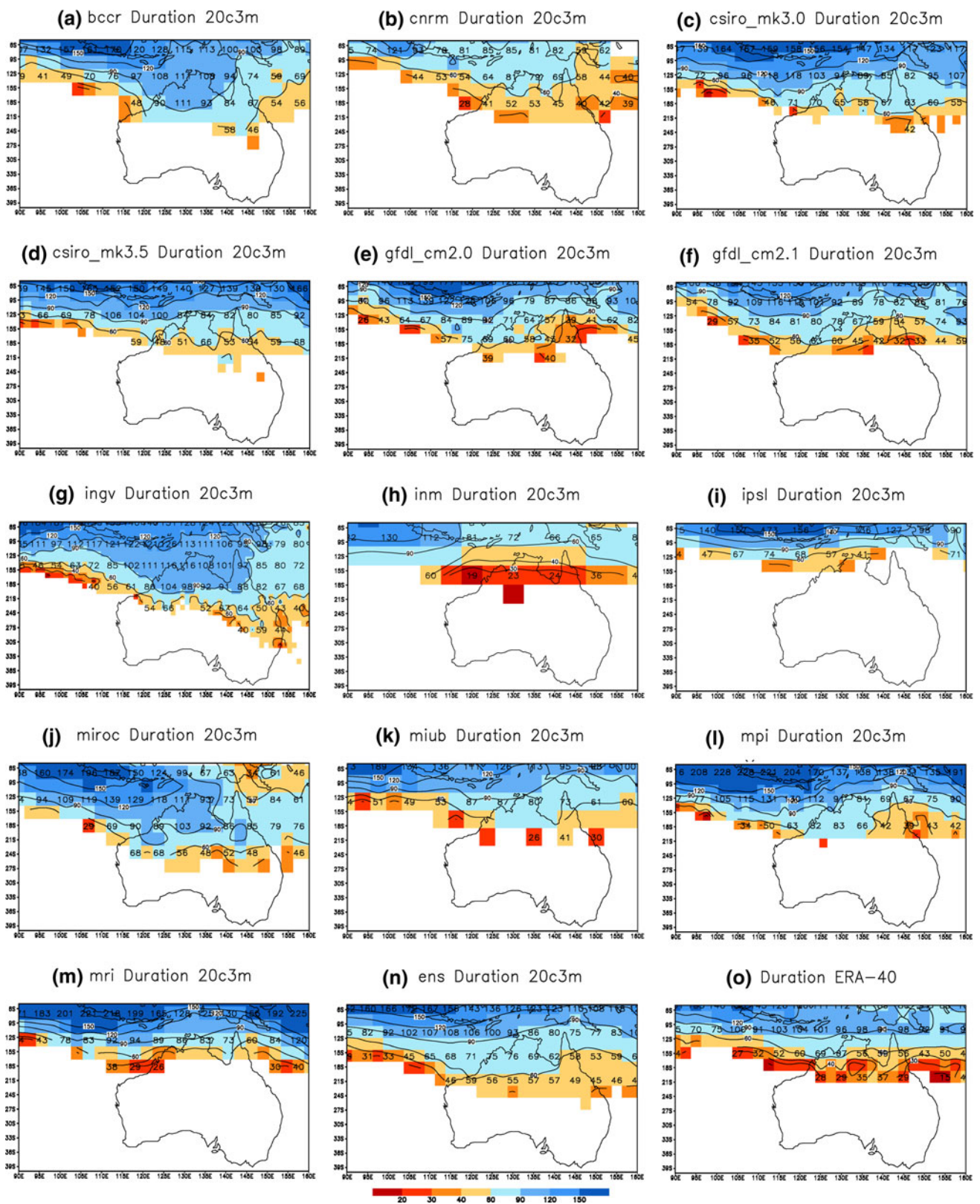
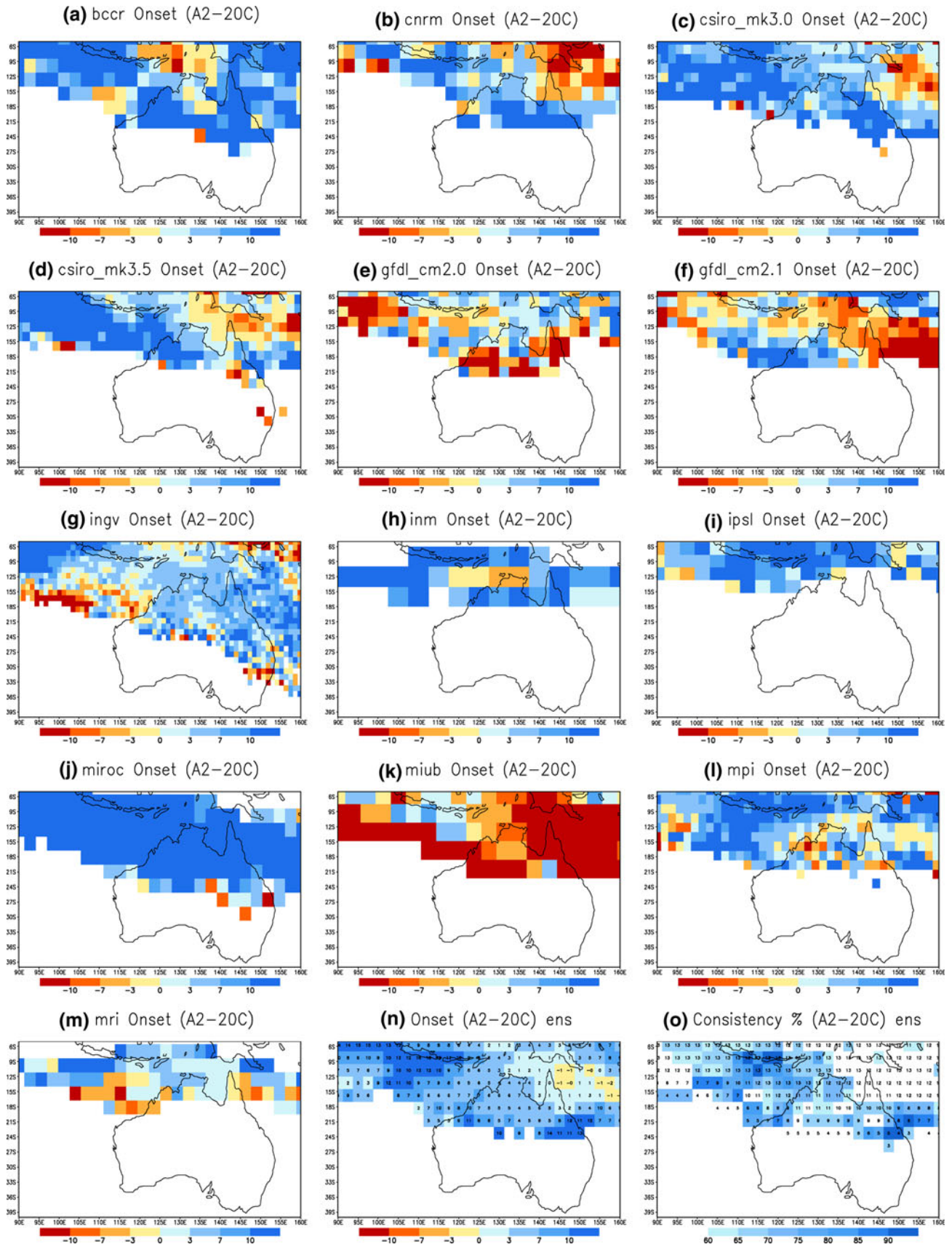


Fig. 2 As Fig. 1 but for the duration of Australian monsoon (unit: days)



◀ **Fig. 3 a–m** Changes in Australian monsoon onset (unit: days) between the model 20-year A2 (2081–2100) and 20C3 M simulations. **n** 13-model ensemble results after regridding the model data into common 2.5° by 2.5° resolution; **o** consistency (%) measured by the percentage of the number of models which simulated the same sign as the ensemble changes in **n**

model ensemble results in Fig. 4n display a robust signal of the delayed onset in the northern Australian region by a week or so. From these direct comparisons, we gain our confidence about the robustness of the changes shown in Fig. 3.

Changes in monsoon retreat dates are shown in Fig. 5. There are several different combinations between results in Fig. 3 (onset) and Fig. 5 (retreat) which lead to the changes in monsoon duration (Fig. 6): (1) the models including BCCR, CNRM, GFDL_CM2.0, GFDL_CM2.1 and INGV tend to show either delayed onset with delayed retreat, or early onset with early retreat. For this group of models, this means a shift in the monsoon seasonal cycle but small changes in duration; (2) the models including CSIRO-O_mk3.0, CSIRO_mk3.5 and MRI show delayed onset and early retreat in most locations, implying significant reductions in their monsoon durations; (3) another group of models including MIROC, MIUB and MPI, showing earlier monsoon retreat over a large part of the ocean and delayed monsoon retreat over land.

There is good agreement among the models over the southern Sumatra and Java region where the majority simulates shortened monsoon duration by 7–10 days. Poor model agreement exists over the tropical Australian continent (ref. Fig. 6o). For example, the BCCR, GFDL_cm2.0, MIROC and MIUB models simulate longer durations while the CNRM, CSIRO_mk3.5 and MRI models show shorter duration. The relatively small changes in duration in tropical Australian land shown in the model ensemble results in Fig. 6n do not at all suggest that the monsoon duration does not change in future climate. Rather, this is caused by large uncertainties in the model projections because the models are significantly divided over the sign of the changes in their simulations. In the tropics, shorter durations occur due to early retreat on top of delayed onset (CSIRO_mk3.0 and mk3.5, INGV, INM, MIROC, MPI and MRI); the delayed onset exceeding the delay of retreat (CNRM and IPSL); and early retreat exceeding early onset (MIUB). The shortened duration of the tropical monsoon together with the projected increases in summer rainfall (e.g. Solomon et al. 2007) implies an enhanced rainfall intensity.

To further assess how the changes in monsoon onset/retreat dates correspond to changes in wind and moisture seasonality, Fig. 7 shows the area-averaged seasonal cycles of rainfall, 850 hPa zonal wind and precipitable water over

two domains: one over the tropics of 100–120°E and 12–5°S where the models agree well on the delayed onset and early retreat; the other over the top end of the Australian continent (120–120°E, 17.5–10°S) where there is a lack of agreement. As discussed in Zhang et al. (2012), global warming leads to increases in *PW* following the Clausius-Clapeyron relationship but the normalized *PW* (Fig. 7a, d), which is used in defining onset/retreat, does not undergo significant changes. This is largely because it measures the relative changes in *PW* seasonality, rather than *PW* itself. In both regions, the changes in *PWn* are less than ± 0.1 , which, as pointed out by Zhang (2010), have little effect on onset/retreat dates. Rather the changes are in good agreement with significant reductions of the westerly wind in the tropics (Fig. 7b). Under global warming, models that simulate delayed onset also simulate significant reductions of westerlies from middle September to early April. Models that do not agree well on the extent of wind changes over the top end of the Australian continent, they do not agree on the likely changes in monsoon onset over land. In the tropical region, changes in rainfall (Fig. 7c) also suggest delayed start and early termination of the monsoon rainy season, corresponding to significant rainfall reductions at the beginning and the end of the monsoon. This is accompanied by enhanced rainfall intensity during the monsoon season reflected by the increases in 95 percentile rainfall distributions in the A2 experiments (not shown). This leads to an increase in averaged total rainfall (c.f. Colman et al. 2011; Moise et al. 2012). This is also consistent with other studies of increased rainfall intensity under global warming (e.g. Sun et al. 2007; Trenberth 2011).

3.3 Underlying mechanism for the changes in onset/retreat

We now focus on exploring the underlying processes leading to such model-simulated results in Sect. 3.2. First of all, we need to identify key processes governing the monsoon variations in these models before we discuss the likely processes leading to its responses to global warming. A large number of studies have shown a significant influence of the El Niño-Southern Oscillation (ENSO) on the Australian summer monsoon. Joseph et al. (1991) found warm SSTs in the eastern Pacific Ocean and cool SSTs north of Australia were related to delayed onset. Drosowsky (1996) showed significant negative correlations between Darwin monsoon onset and the Southern Oscillation Index (SOI). Smith et al. (2008) documented a similar relationship between rainy season onset in northern Australia and the SOI. A recent study by Taschetto et al. (2010) identified delayed onset and early retreat of the Australian monsoon associated with a specific SST pattern known as El Niño

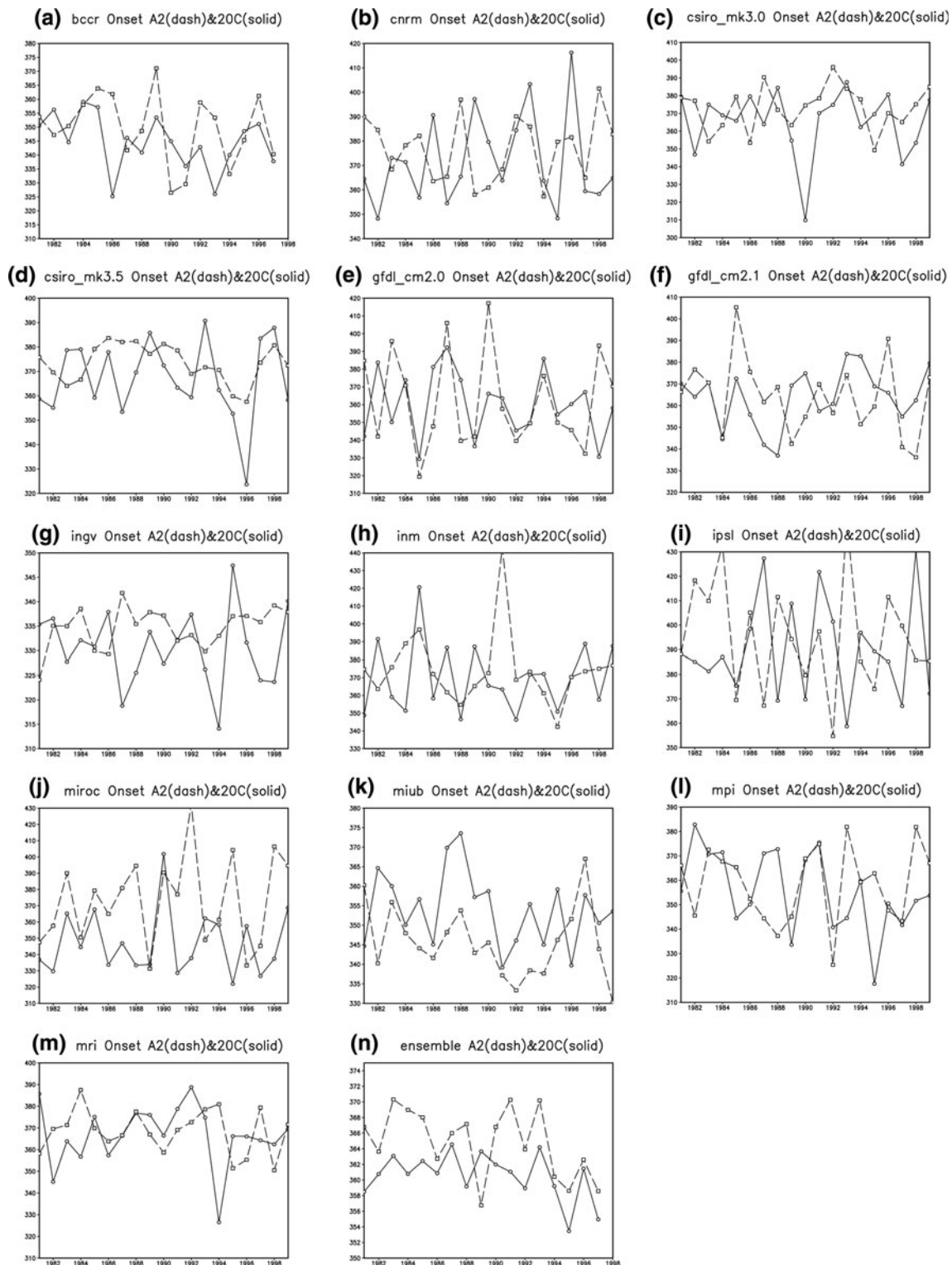


Fig. 4 a–m time series of area-averaged monsoon onset (unit Julian Day) in the *top end* of the Australian continent (120–140°E and 17.5–10°S) in the 13 CMIP3 models in their A2 (*dashed line*) and 20C3 M (*solid line*) simulations; **n** the 13-model ensembles of results from **a** to **m**

Modoki. Here, Fig. 8 shows the correlations between model area-averaged onset dates over northern Australia (the same domain as used in Fig. 7) and November surface

temperatures. The contour line in the diagram represents the 95 % confidence level (bearing in mind that it is only an indicative measurement with such a small sample size).

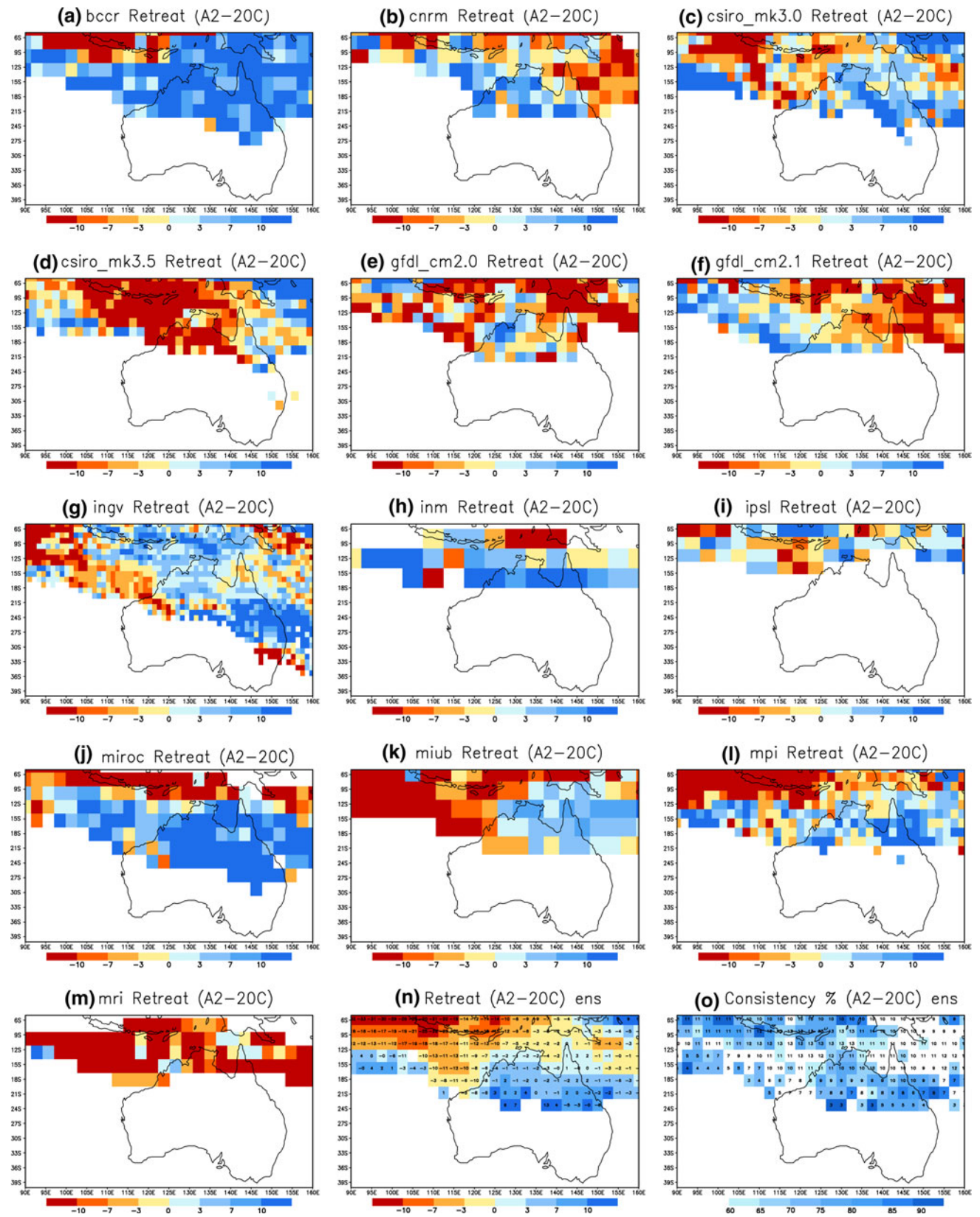


Fig. 5 As Fig. 3 but for changes in monsoon retreat

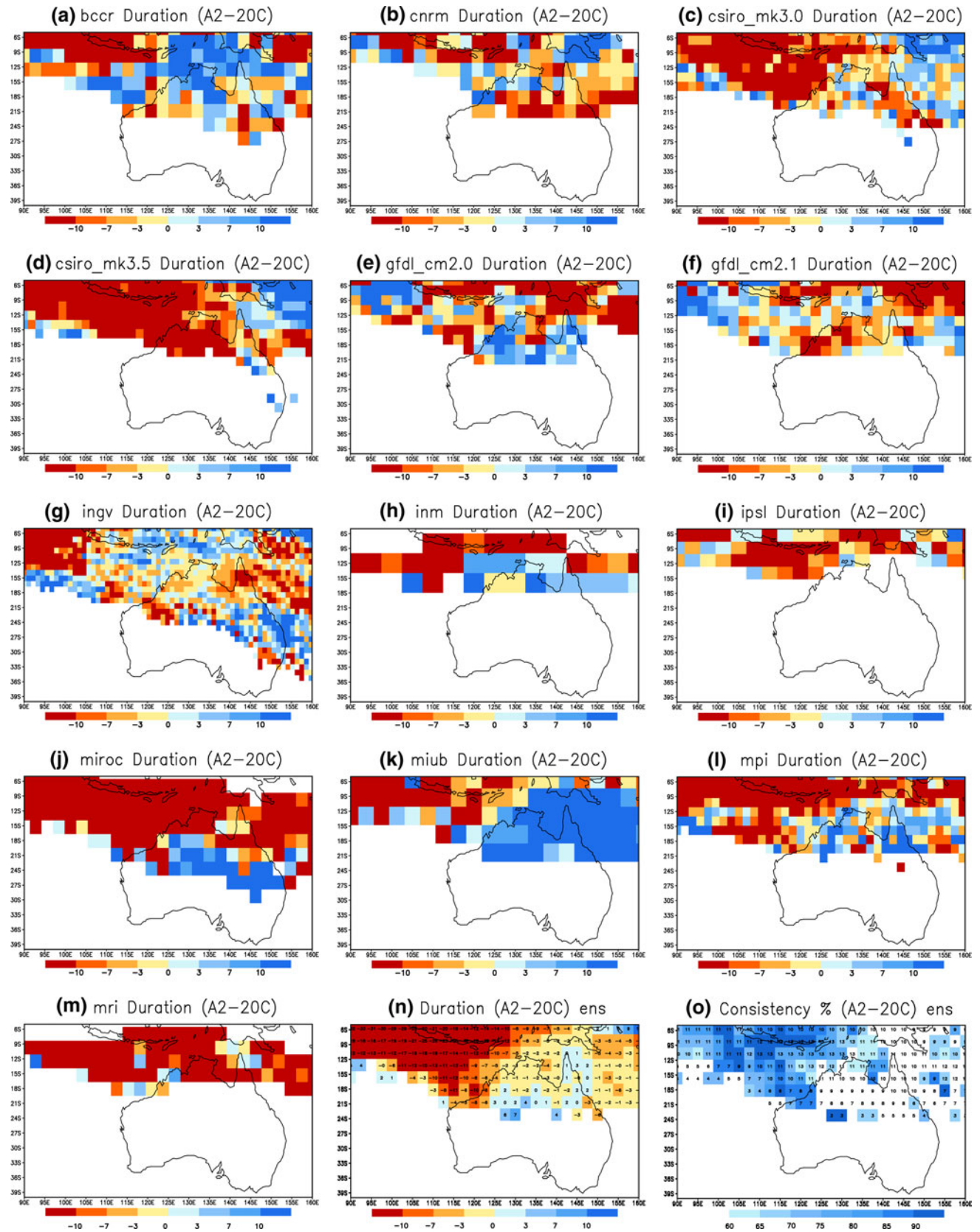


Fig. 6 As Fig. 3 but for changes in monsoon duration

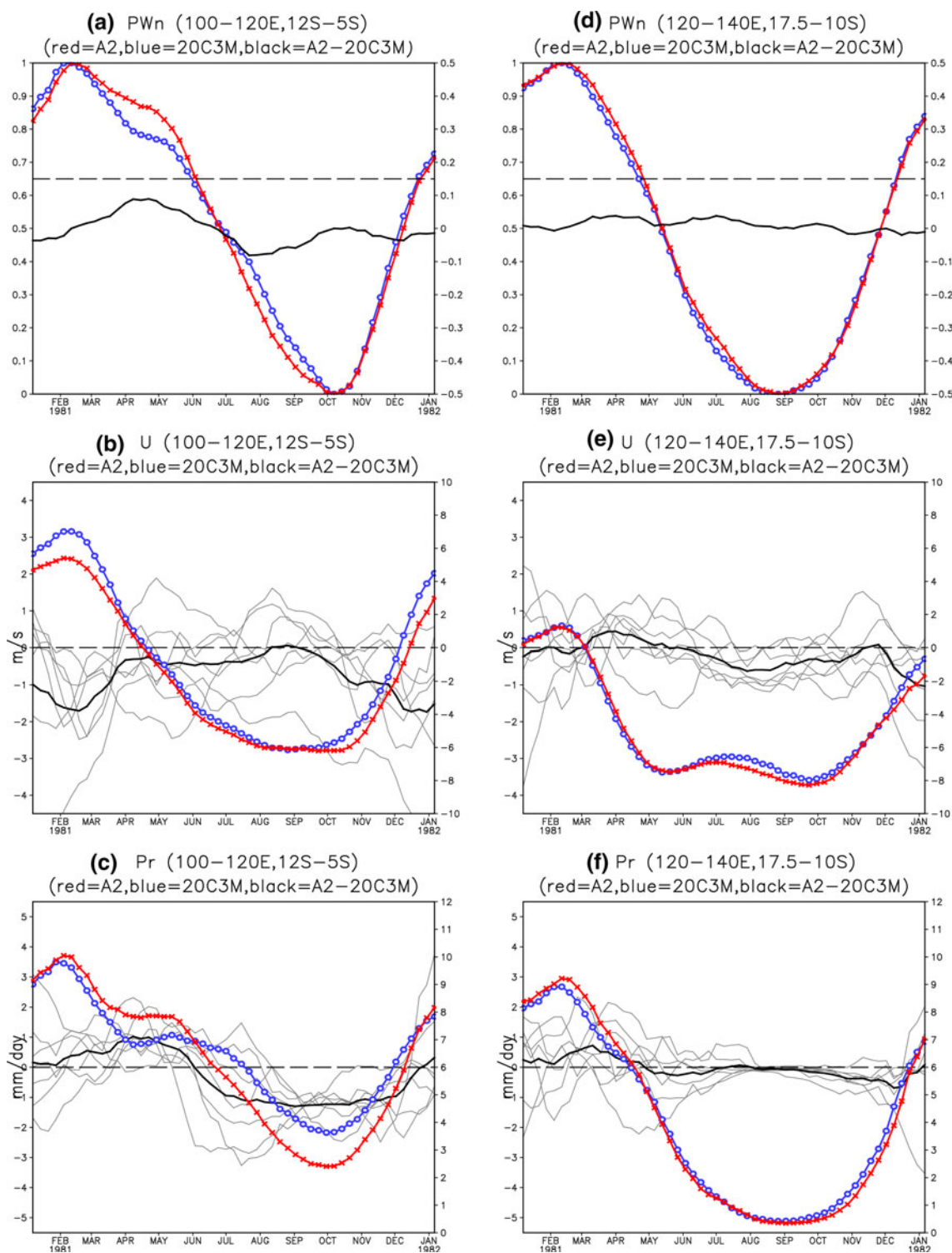


Fig. 7 13-model ensembles of normalised precipitable water (*PWn*), zonal wind and rainfall seasonality over the areas of 100–120°E and 12–5°S (**a–c**) and 120–140°E and 17.5–10°S (**d, e**). **a** Daily *PWn* climatology with blue line showing 20-year 20C3 M results and red line showing A2 simulations. Black line with secondary y axis (on the

right) shows the changes in *PWn* between A2 and 20C3 M results; **b** as **a** but for 850 hPa zonal wind, with grey lines showing results from models simulating delayed onset; **c** as **a** but for rainfall (mm day⁻¹). **d, e** are as **a–c** but for the averages over the top end of the Australian continent

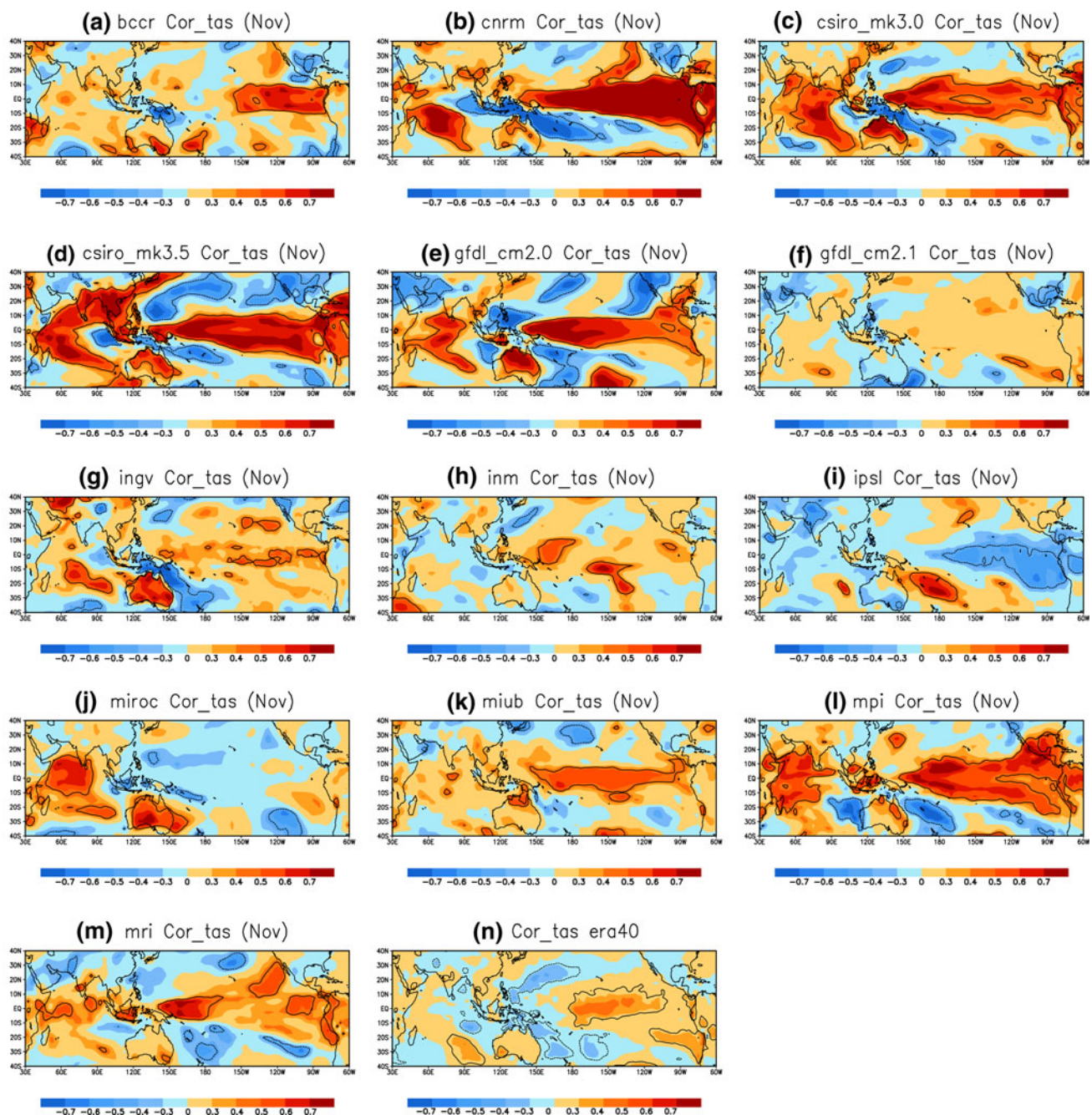


Fig. 8 a–m Correlations between 20-year monsoon onsets averaged over the region of 120–140°E and 17.5–10°S and surface temperature in November in each of the CMIP3 model 20C3 M results over the period of 1981–2000. *Contour lines* indicate the correlations are

significant at 95 % confidence level. **n** Correlations calculated between onset dates from 43-year (1959–2001) ERA-40 reanalysis data and observed GISST sea surface temperature data in November

A number of features stand out. First of all, 8 of the 13 models exhibit strong El Niño-like patterns similar to those identified using ERA-40 reanalysis data (Fig. 8n). In these models (BCCR, CNRM, CSIRO_mk3.0, CSIRO_mk3.5, GFDL_cm2.0, MIUB, MPI and MRI), positive correlations occur over the eastern and central Pacific which suggest delayed onsets occur with these El Niño-like SST conditions. The second feature is that, apart from the MIUB

model, onset dates are negatively correlated with surface temperatures to the north of Australia, near Sumatra/Java and over the Java and Timor Seas. This analysis confirms the influence of regional SSTs north of Australia as found in previous studies (e.g. Joseph et al. 1991; Li et al. 2011).

This analysis also shows that the onset of the Australian monsoon is closely related to SSTs in the Indian Ocean. More than half of the models show onset-SST correlation

patterns over the Indian Ocean which, to some extent, resemble the Indian Ocean Dipole (IOD) (Saji et al. 1999). In these models, delayed onset is associated with cool SSTs in the eastern part of the Indian Ocean nearby the Sumatra-Java archipelago and warm SSTs in the western part of the Indian Ocean. This IOD-like correlation pattern is most obvious during October and November but not other months. Not surprisingly, no such correlation is seen with monsoon retreat dates since the IOD peaks during SON and then decays rapidly thereafter (Saji et al. 1999). Models including CNRM, CSIRO_mk3.0, CSIRO_mk3.5, GFDL_cm2.0, MPI and MRI, which show strong El Niño-like patterns in the tropical Pacific, also display the IOD-like patterns. A few models (INGV and MIROC) exhibit IOD-like patterns but no El Niño-like patterns.

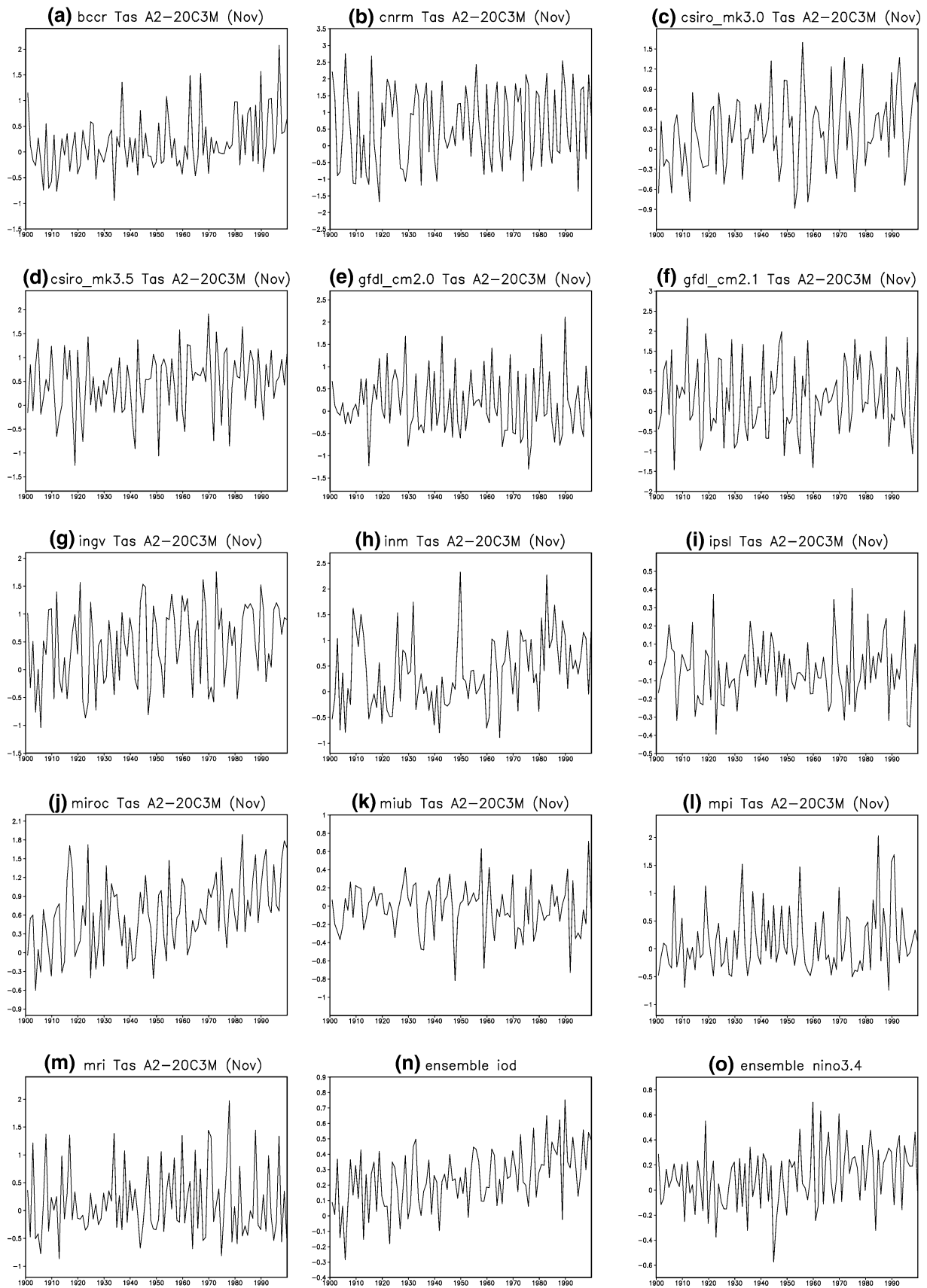
To further examine the possible linkage between IOD and the monsoon onset in this domain, we have calculated the correlations between modeled onset dates and monthly IOD index from the thirteen models. The IOD index is calculated as the sea surface temperature differences averaged over 50–70°E and 10°S–10°N in the west and 90–110°E and 10°S to 0 in the east as defined in Saji et al. (1999). Apart from four models (BCCR, GDSL_cm2.1, IPSL and MIUB), most models exhibit positive correlations between the IOD values and onset dates. This is also seen in the ERA40 data. While studies have shown some degree of independence of the IOD (e.g. Saji et al. 1999; Behera et al. 2006) and the possibility that IOD could even influence the ENSO development (e.g. Luo et al. 2010), it is well known that ENSO influences the Indian Ocean SSTs. Thus, to account for this, we have calculated the partial correlations between onset dates and the IOD values after firstly removing the influence of Niño3.4 SSTs (ref. Zhang and Zhang 2010). We find that the correlations between the IOD values and onset dates remain largely unchanged in most models. These results highlight the role of Indian Ocean to the Australian monsoon studies even though recent studies have focused on its importance in affecting southeast Australian rainfall (Cai et al. 2009a, b; Ummenhofer et al. 2009).

Given the importance of Pacific and Indian Ocean SSTs in influencing variations of the monsoon in the CMIP3 models, we now assess the linkage between SST warming in the CMIP3 models and the model-simulated changes in monsoon onset/retreat. Many studies analysing CMIP3 model simulations have noted that mean SST changes display weak 'El Niño-like' structures, with sea surface temperatures in the central and east equatorial Pacific warming more than those in the west. However, there was no consistent indication of discernible changes in projected ENSO amplitude or frequency (cf. Collins et al. 2010). We found that (not shown) in the 13 models the projected SST warming patterns are less clear in the Pacific prior to the

Australian monsoon onsets, with only three models having a larger warming tendency in the tropical eastern Pacific Ocean. Although the Australian summer monsoon onset is strongly influenced by ENSO-related SST conditions in the Pacific as shown in Fig. 8, there is a lack of coherence between the pattern of tropical Pacific SST warming and onset/retreat changes cross the models, suggesting there likely are other candidates that contribute to the model-simulated changes in monsoon onset/retreat in this region.

In contrast, there are quite a few models showing relatively weak warming in the eastern Indian Ocean (including BCCR, CNRM, CSIRO_mk3.0, CSIRO_mk3.5, INGV and INM) or stronger warming in the western part of the Indian Ocean (MIROC). All of these models point to a positive IOD-like pattern in their mean SST warming structure. Prompted by more detailed analyses from Cai et al. (2009c) which reported an overall increase of positive IODs in CMIP3 models under global warming, here we plot out the changes in November monthly IOD index from the 13 models in their 100-year 20C3 M and A2 integration (Fig. 9). About nine models show positive trends and the multi-model ensemble (Fig. 9n) increases rapidly in the latter part of the 100-year period (cf. Cai et al. 2009c). As a reference to compare this warming pattern with the warming in the Pacific, Fig. 9o also shows the model ensemble mean of the SST warming over the Niño3.4 region (190–270°E and 5°S–5°N) against the warming in the western Pacific (130–190°E and 5°S–5°N). While there is a tendency for more El Niño-like warming, this is much weaker than that of IOD. Furthermore, there is a degree of coherence between changes shown in Fig. 3, correlations shown in Fig. 8 and results shown in Fig. 9. For example, the CNRM, CSIRO_mk3.0 and 3.5, MIROC, MPI and MRI models show dipole correlation patterns in the Indian Ocean which strengthen under global warming. These models also simulate delayed onset of the monsoon. In some models (e.g. GFDL_cm2.0, GFDL_cm2.1 and MIUB) there is either a lack of any strong SST correlation patterns in the Indian Ocean (GFDL_cm2.1, IPSL and MIUB) or else the trend of the patterns is not significant (GFDL_cm2.0, GFDL_cm2.1 and IPSL). For these models, they tend to show somewhat different results in the changes in monsoon onset. These results suggest that the Indian Ocean SST responses to global warming are important features affecting the changes in the monsoon onset. This agrees with the observational analysis of Joseph et al. (1991), which showed the impact of Indian Ocean SSTs on the onset of the Australian summer monsoon.

As the definition of monsoon onset involves both the atmospheric moistening process (represented by normalized *PW*) and the atmospheric dynamics (represented by zonal wind), we examine the contribution of the changes in regional circulation to the model-simulated changes in



◀ **Fig. 9 a–m** Changes in monthly Indian Ocean Dipole index (see text for definition) simulated by the 13 CMIP3 models during the 100-year 20C3 M and A2 simulations. **n** 13-model ensembles from **a** to **m**; **o** same as **n** but for the relative changes in Nino3.4 monthly SST (190–270°E 5°S–5°N) against the SST in the Western Pacific (130–180°E, 5°S–5°N)

onset/retreat. Figure 10 shows correlations between averaged onset dates over the top end of the Australian continent and November 850 hPa zonal wind. Very similar patterns are seen if one uses the onset dates averaged over the tropical domain or uses October/December wind data. Strong correlations are seen over the tropics including the eastern Indian Ocean, the Sumatra-Java islands and nearby warm waters. Nevertheless, there are a few models (BCCR, GFDL_cm2.1, INM and IPSL) which show only a weak influence of pre-monsoon westerly winds on monsoon onset. With global warming, the patterns of the changes in the 850 hPa wind (Fig. 11) overall agree well with the correlation pattern in Fig. 10. The CNRM, CSIRO_mk3.0, CSIRO_mk3.5, INGV, INM, MIROC, MPI and MRI models all simulate significant reductions of the westerly wind in the tropical eastern Indian Ocean and over Sumatra-Java and nearby regions, with a consequent delay of the monsoon onset dates. Both GFDL models simulate enhanced westerlies and consequent earlier onsets (Fig. 3e, f).

Smith et al. (2012) noted that there was a tendency for tropical zonal winds to decrease slightly under global warming and that this could be understood in terms of a general weakening of the global circulation in response to global warming. Furthermore, there are large body of studies showing the weakening of Walker circulation in the Indo-Pacific domain (Vecchi et al. 2006; Power and Smith 2007) and the consequence of El Nino-like changes in mean-state SSTs in the tropical Pacific on the eastward shift of Walker circulation etc. (Yamaguchi and Noda 2006; Solomon et al. 2007). All these can contribute to the zonal wind anomalies in Fig. 11, which by and large exhibit easterly anomalies in the eastern Indian Ocean and maritime continent and accompanied by westerly anomalies to its east.

Furthermore, reduced westerlies in the eastern Indian Ocean are consistent with a positive IOD-like mean SST warming pattern. As Guan et al. (2003) and Behera et al. (2006) showed that positive IOD SST patterns could also induce easterly anomalies in the tropical eastern Indian Ocean and over Sumatra-Java islands. Indeed, Fig. 12 shows that in most models and the observations (ERA40 data) a positive IOD pattern corresponds to easterly anomalies in the eastern Pacific and nearby Sumatra-Java region. Therefore, the easterly wind anomalies in Fig. 11 in the eastern Indian Ocean and maritime continent can also

be contributed by the upward trend in the modeled IOD SST patterns.

Note that although precipitable water (*PW*) increases with global warming, we found the changes in normalized *PW* (*PW_n* as used in our definition of monsoon onset) lie in the range of ± 0.1 in the monsoon region. There was a lack of correspondence between changes in *PW_n* and changes in monsoon onset or retreat in these models. Nevertheless, we must emphasize that the changes in atmospheric moisture content do affect the characteristics of monsoon rainfall distributions. As shown in Fig. 7, rainfall intensity is increased following the establishment of monsoon circulation and moisture enhancement. We have calculated the changes in 95 percentile rainfall and most models simulate an increase in extreme rainfall amount in the Australian monsoon region.

4 Conclusion and discussions

We have used the method of Zhang (2010) to analyze the results from 13 CMIP3 models in simulating Australian summer monsoon onset, retreat and duration and their potential changes in future climate. The monsoon domain covers south Sumatra and Java region in the tropics and extends to the northern Australian continent. The broad patterns of the onset and evolution of the Australian summer monsoon were, by and large, well captured by the majority of the CMIP3 models. The prominent northwest-southeastward propagation of the Australian summer monsoon starting from south Sumatra-Java region and progressing towards the Australian continent appeared to be a common feature in most of the models. Although the 13-model ensemble gave a remarkable agreement with the onset dates derived from observations, this could be misleading as there were large inter-model discrepancies, with some models simulating much earlier onset dates while some simulated much late onset. The extent of monsoon inland penetration was also different, with a number of models not indicating any southward intrusion toward the interior region.

The agreement on the changes in onset/retreat due to global warming varied significantly across the domain. The majority (over 80 %) of the models simulated a delayed onset by about 10 days in the tropics including southern Sumatra-Java region and part of the top end of the Australia continent, but the model results diverged over the inland region where the model ensembles suggested some delay, but with less agreement. Different combinations of changes in onset and retreat were identified, with one group of the models showing similar changes to both onset and retreat and with relatively small changes in monsoon duration. Another group of models had delayed onset and

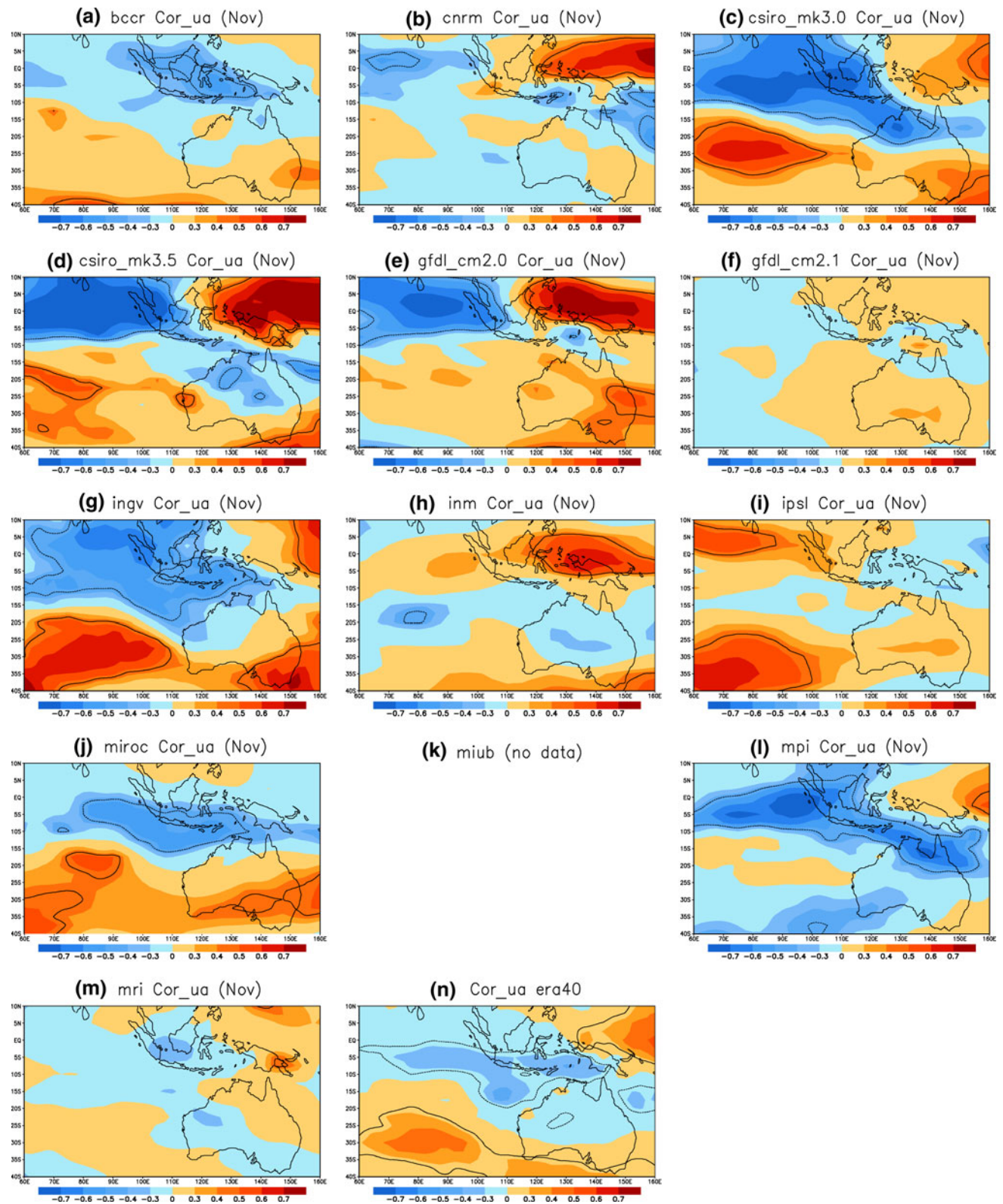


Fig. 10 As (8) but for correlations between monsoon onset and zonal wind at 850 hPa. The model MIUB (k) data are not available for the analysis

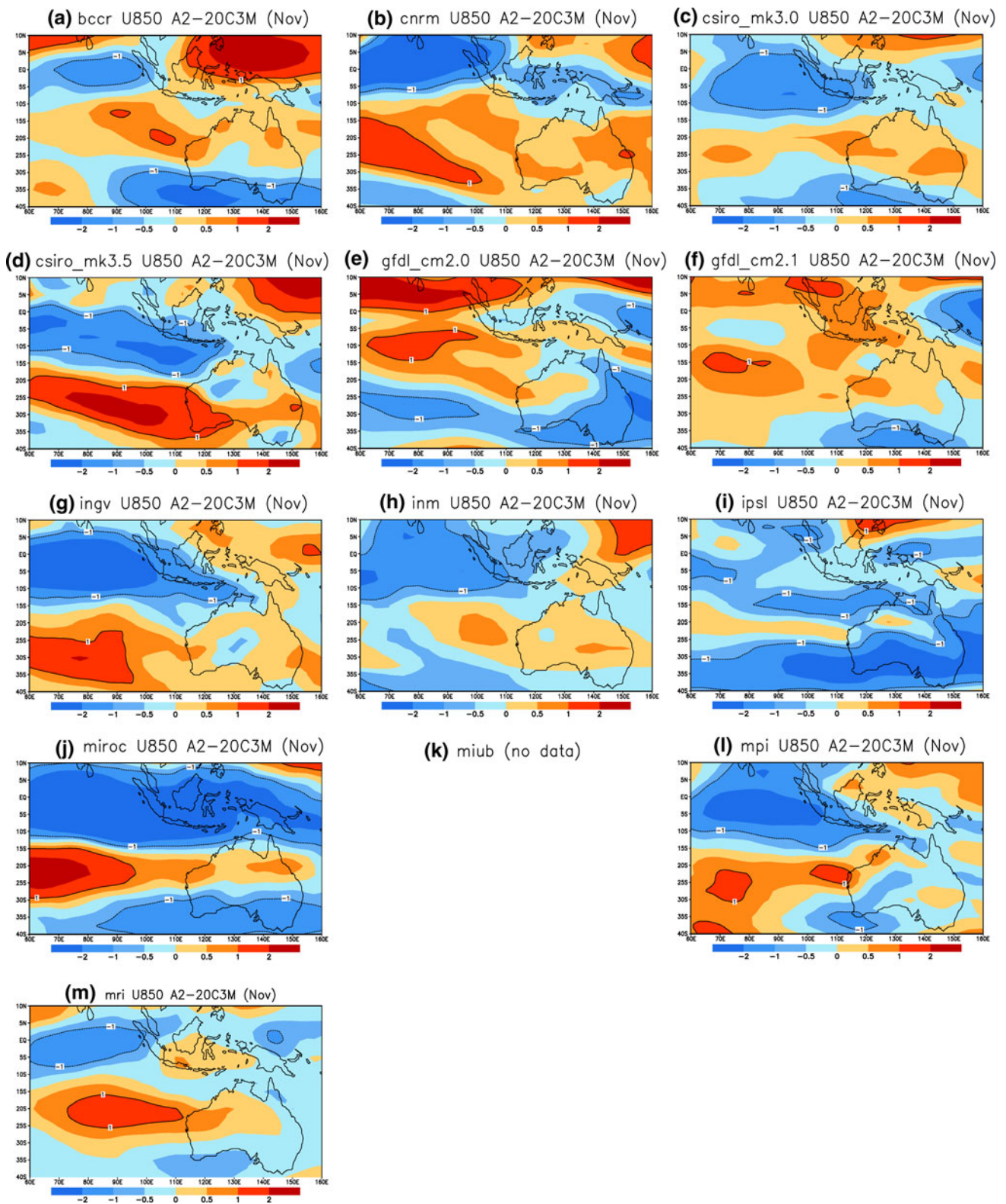


Fig. 11 a–m Changes in 850 hPa zonal wind (mm s^{-1}) simulated by the 13 CMIP3 models during the 20-year 20C3 M and A2 simulations analysed in this study

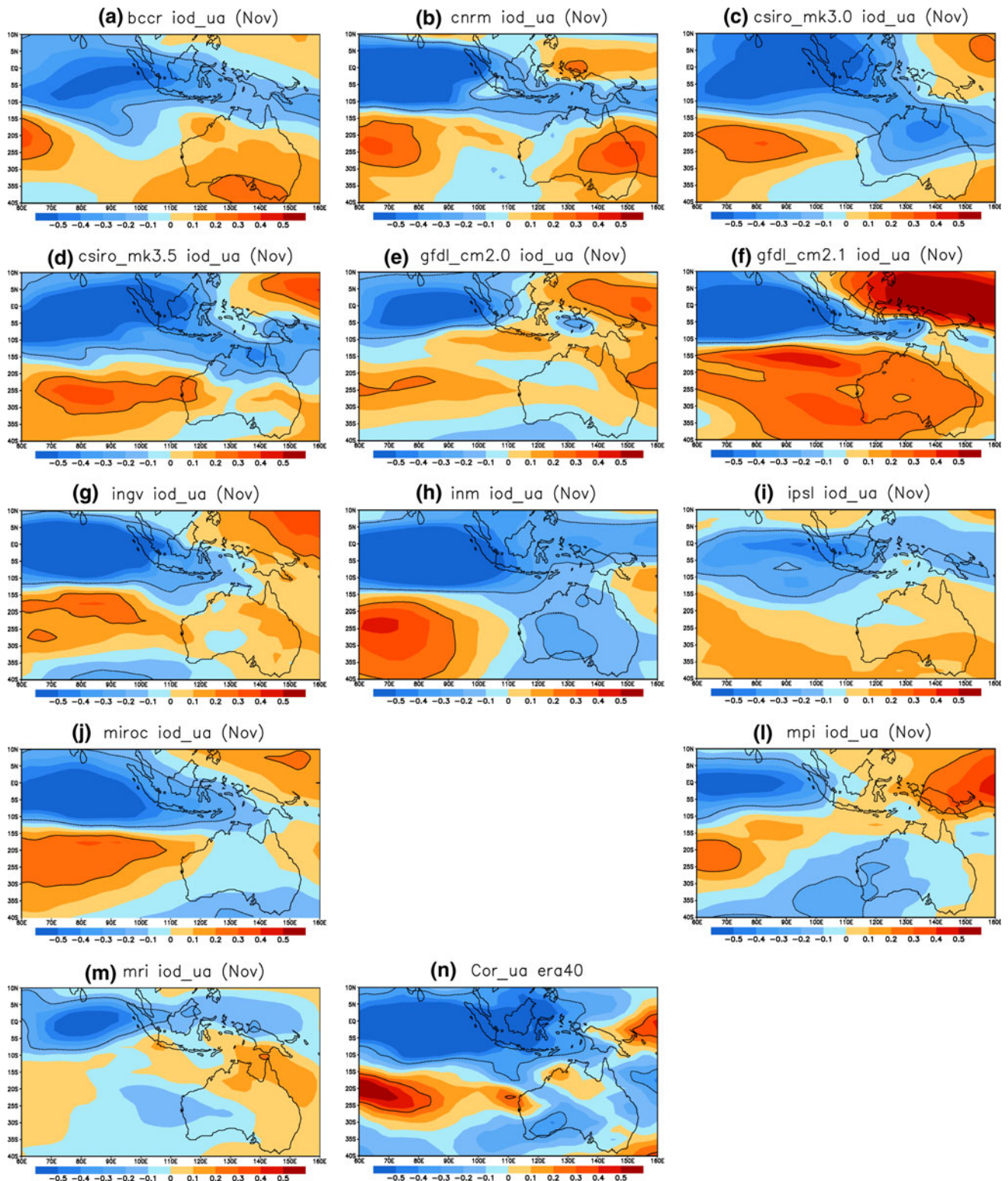


Fig. 12 a–m Partial correlations between monthly IOD index and zonal wind in November from 12 of the thirteen models in the 20-year 20C3 M experiments (no data from MIUB). These correlations are calculated after removing the influence of ENSO which is represented

by Niño 3.4 SSTs in the models; n the same correlations derived from ERA40 wind and observed SSTs for the period of 1959–2001. Contour lines indicate the correlations are significant at 95 % confidence level

early retreat in most locations with consequent reduction in monsoon duration. We also found some models showed different changes in monsoon onset/retreat over land and ocean. Consequently, the model agreement on the changes in monsoon duration in the tropical Australia is poor. Using the daily data, we have reported some different results to the ones found by analyzing monthly data. For instance, the shortened duration derived from this analysis is contradictory to the study of Moise et al. (2012) in which they suspected prolonged tropical Australian monsoon season based on the increases in rainfall in April/May. Based on our analysis, such increases could be caused by the increase in atmospheric moisture condition rather than the strengthened monsoon circulation.

Of the 13 models, 8 of them captured the ENSO-like correlations between pre-monsoon SSTs and onset/retreat dates correlation patterns, evident in the observations. The remainder showed no such patterns. However, changes in monsoon onset/retreat dates were not found to be related to changes in Pacific SSTs. In stead, changes in both the tropical Walker circulation and the IOD-like SST changes appear to be important. The main cause of the simulated delayed onset was associated with the reduction of simulated westerlies (ref. Fig. 11) during the pre-monsoon season. This implied weakening of the Walker circulation in the Indo-Pacific domain in response to global warming as discussed elsewhere (e.g. Vecchi et al. 2006; Power and Smith 2007). Most models simulated easterly anomalies in the eastern part of the tropical eastern Indian Ocean, nearby Sumatra-Java islands and warm water. To their east, they showed westerly anomalies. The combined effect of these two anomalies pointed to a reduced low-level convergence associated with weakened ascending motion of Walker circulation in the region. In addition, the reduced westerly over eastern tropical Indian Ocean and nearby Sumatra/Java was also associated with the upward trend in the positive IOD SST patterns in these models. Studies such as Guan et al. (2003) and Behera et al. (2006) showed that positive IODs were able to generate easterly anomalies in the region. Partial correlations between IOD and zonal wind in the CMIP3 models after removing the ENSO impacts further confirmed such connections in these models. Regardless of the unresolved arguments on the IOD-ENSO (in)dependence and complex cause-effect relationship between wind and SST anomalies in the tropical Indian Ocean, our results suggest that the Indian Ocean needs to be considered when estimating changes in the Australian summer monsoon in a future climate.

There are a number of important issues which have not been explored in this analysis. First of all, a large number of studies underline the influence of the MJO on the Australian summer monsoon onset and its rainfall variations (e.g. Hung and Yanai 2004; Wheeler and McBride

2005; Wheeler et al. 2009). Given that one key result in this analysis is the recognition of the influence of the Indian Ocean SST warming pattern on changes in Australian summer monsoon onset/retreat, clearly we need to explore further how much of these changes in onset/retreat is directly linked to the MJO activities which originate in the Indian Ocean (Wheeler and Hendon 2004) and the skills of the models in capturing the intraseasonal variations associated with MJO. Secondly, studies such as Zhang and Zhang (2010) identified potential impacts of Asian winter monsoon on the Australian summer monsoon climate. It is still unclear whether the weakening of the Asian winter monsoon (e.g. Chang et al. 1979; Zhang and Zhang 2010) has contributed to the delayed onset of Australian summer monsoon associated with cold surge in the Northern Hemisphere. In addition, in the analysis we have simply examined the regionalized features of mean SST warming and have not examined how the potential changes in SST interannual variations affect the monsoon onset/retreat (e.g. Cai et al. 2009b). How continental warming contributes to the monsoon responses to climate change is another important issue we have not discussed here. A recent study of Kullgren and Kim (2006) has underlined the importance of pre-monsoon thermal lows in triggering the onset of the Australian monsoon. Finally, while we have been able to document differences in CMIP3 model-simulated changes in monsoon onset/retreat, we have not investigated what have caused such different mechanisms operating in these models. All these issues need further investigations to improve our knowledge of how the monsoon system responds to global warming.

Acknowledgments Dr. P Liang's visit to CAWCR for participating in the analysis was supported as part of the collaboration agreement the Australian Bureau of Meteorology and China Meteorological Administration and by "National Natural Science Foundation of China under Grant No.40875056". The authors appreciate discussions with Drs. H. Hendon, M. Wheeler, R. Colman, and J. Brown on the preliminary results. Detailed comments from Dr. J Brown and L. Qi during the internal review process are acknowledged. We acknowledge the modelling groups, the Program for Climate Model Diagnosis and Intercomparison (PCMDI) and the WCRP's Working Group on Coupled Modelling (WGCM) for their roles in making available the WCRP CMIP3 multi-model dataset. Support of this dataset is provided by the Office of Science, US Department of Energy. The authors sincerely thank the two anonymous reviewers for the very thoughtful comments and suggestions.

References

- Aldrian E, Susanto RD (2003) Identification of three dominant rainfall regions within Indonesia and their relationship to sea surface temperature. *Int J Climatol* 23(12):1435–1452
- Behera SK, Luo JJ, Masson S, Rao SA, Sakuma H, Yamagata T (2006) A CGCM study on the interaction between IOD and ENSO. *J Clim* 19:1688–1705

- Cai W, Cowan T, Sullivan A (2009a) Recent unprecedented skewness towards positive Indian Ocean Dipole occurrences and its impact on Australian rainfall. *Geophys Res Lett* 36:L11705. doi: [10.1029/2009GL037604](https://doi.org/10.1029/2009GL037604)
- Cai W, Sullivan A, Cowan T (2009b) Rainfall teleconnections with Indo-Pacific variability in the WCRP CMIP3 models. *J Clim* 22:5046–5071
- Cai W, Cowan T, Sullivan A (2009c) Climate change contributes to more frequent consecutive positive Indian Ocean Dipole events. *Geophys Res Lett* 36:L23704
- Chang CP, Krishnamurti TN (eds) (1987) *Monsoon meteorology*. Oxford University Press, Oxford
- Chang CP, Erickson JE, Lau KM (1979) Northeasterly cold surges and near-equatorial disturbances over the winter MONES area during Dec. 1974. Part I: Synoptic aspects. *Mon Weather Rev* 107:812–829
- Chen LX, Zhu QG, Luo HB (1991) *East Asian Monsoon* (in Chinese). China Meteorological Press, China
- Collins M et al (2010) The impact of global warming on the tropical Pacific Ocean and El Niño. *Nat Geosci* 3:391–397
- Colman RA, Moise AF, Hanson L (2011) Tropical Australian climate and the Australian monsoon as simulated by 23 CMIP3 models. *J Geophys Res* (in press)
- Drosowsky W (1996) Variability of the Australian Summer Monsoon at Darwin: 1957–1992. *J Clim* 9:85–96
- Guan Z, Ashok K, Yamagata T (2003) Summertime response of the tropical atmosphere to the Indian Ocean Dipole sea surface temperature anomalies. *J Meteorol Soc Jpn* 81:533–561
- Hendon H, Liebmann B (1990) A composite study of onset of the Australian summer monsoon. *J Atmos Sci* 47:2227–2240
- Holland GJ (1986) Interannual variability of the Australian summer monsoon at Darwin: 1952–82. *Mon Weather Rev* 114:594–604
- Hung C-W, Yanai M (2004) Factors contributing to the onset of the Australian summer monsoon. *Q J R Meteorol Soc* 130:739–758
- Joseph PV, Liebmann B, Hendon HH (1991) Interannual variability of the Australian summer monsoon onset: possible influence of Indian summer monsoon and El Niño. *J Clim* 4:529–538
- Kajikawa Y, Wang B, Yang J (2009) A multi-time scale Australian monsoon index. *Int J Climatol*. doi: [10.1002/joc.1955](https://doi.org/10.1002/joc.1955)
- Kim KY, Kullgren K, Lim GH, Boo KO, Kim BM (2006) Physical mechanism of the Australian summer monsoon: 2. Variability of strength and onset and termination times. *J Geophys Res* 111:D20105. doi: [10.1029/2005JD006808](https://doi.org/10.1029/2005JD006808)
- Kim HJ, Wang B, Ding Q (2008) The global monsoon variability simulated by CMIP3 coupled climate models. *J Clim* 21:5271–5294
- Kitoh A, Uchiyama T (2006) Changes in onset and withdrawal of the East Asian summer rainy season by multi-model global warming experiments. *J Meteorol Soc Jpn* 84:247–258
- Kullgren K, Kim KY (2006) Physical mechanism of the Australian summer monsoon: 1. Seasonal cycle. *J Geophys Res* 111:20104. doi: [10.1029/2005JD006807](https://doi.org/10.1029/2005JD006807)
- Li J, Zeng Q (2003) A new monsoon index and the geographical distribution of the global monsoons. *Adv Atmos Sci* 20:299–302
- Li J, Wu Z, Jiang Z, He J (2010) Can global warming strengthen the East Asia summer monsoon? *J Clim* 23:6696–6705
- Li J, Feng J, Li Y (2011) A possible cause of decreasing summer rainfall in northeast Australia. *Int J Climatol* 31. doi: [10.1002/joc.2328](https://doi.org/10.1002/joc.2328)
- Lin J-L, Weickma KM, Kiladis GN, Mapes BE, Schubert SD, Suarez MS, Bacheister JT, Lee M (2008) Subseasonal variability associated with Asian summer monsoon simulated by 14 IPCC AR4 coupled GCMs. *J Clim* 21:4541–4567
- Luo JJ, Zhang R, Behera SK, Masumoto Y (2010) Interaction between El Niño and extreme Indian Ocean dipole. *J Clim* 23:726–742
- Meehl GA, Covey C, Delworth T, Latif M, McAvaney B, Mitchell JFB, Stouffer RJ, Taylor KE (2007) The WCRP CMIP3 multimodel dataset: a new era in climate change research. *Bull Am Meteorol Soc* 88:1383–1394
- Moise AF, Colman R (2009) Tropical Australian and the Australian monsoon: general assessment and projected changes. In: *Proceeding of the 18th world IMACS/MODSIM congress*, Cairns, Australia, 13–17 July 2009, pp 2042–2048
- Moise AF, Colman RA, Brown JR (2012) Behind uncertainties in projections of Australian tropical climate: analysis of 19 CMIP3 models. *J Geophys Res* (submitted)
- Moron V, Robertson AW, Boer R (2009) Spatial coherence and seasonal predictability of monsoon onset over Indonesia. *J Clim* 22:840–850
- Nicholls N (1984) A system for predicting the onset of the northern Australian wet season. *J Clim* 4:425–435
- Nicholls N (2000) The insignificance of significance testing. *Bull Am Meteorol Soc* 81:981–986
- Nicholls N, McBride JL, Ormerod RJ (1982) On predicting the onset of the Australian wet season at Darwin. *Mon Weather Rev* 110:14–17
- Power SB, Smith IN (2007) Weakening of the Walker circulation and apparent dominance of El Niño both reach record levels, but has ENSO really changed? *Geophys Res Lett* 34:L18702. doi: [10.1029/2007GL030854](https://doi.org/10.1029/2007GL030854)
- Saji B, Goswami N, Vinayachandran PN, Yamagata T (1999) A dipole mode in the tropical Indian Ocean. *Nature* 401:360–363
- Smith IN, Wilson L, Suppiah R (2008) Characteristics of the northern Australian rainy season. *J Clim* 21:4298–4311
- Smith IN, Moise AF, Colman RA (2012) Large-scale circulation features in the tropical western Pacific and their representation in climate models. *J Geophys Res* 117:D04109. doi: [10.1029/2011JD01667](https://doi.org/10.1029/2011JD01667)
- Solomon S et al (2007) Contribution of working group I to the fourth assessment report of the intergovernmental panel on climate change. Cambridge University Press, Cambridge
- Sumi A, Murakami T (1981) Large-scale aspects of the 1978–1979 winter circulation over greater MONEX region, Part I: monthly and season mean fields. *J Meteorol Soc Jpn* 59:625–645
- Sun Y, Solomon S, Dai A, Portmann R (2007) How often will it rain? *J Clim* 20:4801–4818
- Taschetto AS, Haarsma RJ, Gupta AS, Ummenhofer CC, Hill KJ, England MH (2010) Australian monsoon variability driven by a Gill-Matsuno-type response to central west Pacific warming. *J Clim* 23:4717–4735
- Trenberth KE (2011) Changes in precipitation with climate change. *Clim Res* 47:112–138
- Troup AJ (1961) Variations in upper tropospheric flow associated with the onset of Australian summer monsoon. *Indian J Meteorol Geophys* 12:217–230
- Ummenhofer CC, England MH, McIntosh PC, Meyers GA, Pook MJ, Risbey JS, Gupta AS, Taschetto AS (2009) What causes southeast Australia's worst droughts? *Geophys Res Lett* 36:L04706. doi: [10.1029/2008GL036801](https://doi.org/10.1029/2008GL036801)
- Vecchi GA, Soden BJ, Wittenberg AT, Held IM, Leetmaa A, Harrison MJ (2006) Weakening of tropical Pacific atmospheric circulation due to anthropogenic forcing. *Nature* 441:73–76
- Wang B (2006) *The Asian Monsoon*. Springer, Heidelberg
- Webster PJ (2006) The coupled monsoon system. In: Wang B (ed) *The Asian Monsoon*. Springer, New York, vol 3, pp 66–787
- Wentz FJ, Ricciardulli L, Hilburn K, Mear C (2007) How much more rain will global warming bring? *Science* 317:233–235
- Wheeler MC, Hendon HH (2004) An all-season real-time multivariate MJO Index: development of an index for monitoring and prediction. *Mon Weather Rev* 132:1917–1932

- Wheeler MC, McBride JL (2005) Australian-Indonesian monsoon. In: Lau WKM, Waliser DE (eds) *Intraseasonal variability in the atmosphere-ocean climate system*. Praxis. Springer, Berlin, pp 125–173
- Wheeler MC, Hendon HH, Cleland S, Meinke H, Donald A (2009) Impacts of the Madden-Julian oscillation on Australian rainfall and circulation. *J Clim* 22:1482–1498
- Yamaguchi K, Noda A (2006) Global warming patterns over the North Pacific: ENSO versus AO. *J Meteorol Soc Jpn* 84:221–241
- Zeng X, Lu E (2004) Globally unified monsoon onset and retreat indexes. *J Clim* 17:2241–2248
- Zhang H (2010) Diagnosing Australia-Asian monsoon onset/retreat using large-scale wind and moisture indices. *Clim Dyn* 35:601–618
- Zhang CJ, Zhang H (2010) Potential impacts of east Asian winter monsoon on climate variability and predictability in the Australian summer monsoon region. *Theoret Appl Climatol*. doi: [10.1007/s00704-009-0246-2](https://doi.org/10.1007/s00704-009-0246-2)
- Zhang H, Liang P, Moise A, Hanson L (2012) Diagnosing potential changes in Asian summer monsoon onset and duration in IPCC AR4 model simulations using moisture and wind indices. *Clim Dyn* (in press)

Copyright of Climate Dynamics is the property of Springer Science & Business Media B.V. and its content may not be copied or emailed to multiple sites or posted to a listserv without the copyright holder's express written permission. However, users may print, download, or email articles for individual use.